Available online at www.sciencedirect.com
SCIENCE DIRECT®
Carbohydrate Research 340 (2005) 2645–2653
Carbohydrate RESEARCH

Crystal structure and solid-state ^{13}C NMR analysis of *N*-*p*-nitrophenyl-α-D-ribopyranosylamine, *N*-*p*-nitrophenyl-α-D-xylopyranosylamine, and solid-state ^{13}C NMR analysis of *N*-*p*-nitrophenyl-2,3,4-tri-*O*-acetyl-β-D-lyxopyranosylamine and *N*-*p*-nitrophenyl-2,3,4-tri-*O*-acetyl-α-L-arabinopyranosylamine

Andrzej Temeriusz,[a,*] Tomasz Gubica,[a] Paulina Rogowska,[a] Katarzyna Paradowska[b] and Michał K. Cyrański[a]

[a]*Department of Chemistry, Warsaw University, Pasteura 1, Warszawa 02-093, Poland*
[b]*Department of Physical Chemistry, Faculty of Pharmacy, Medical Academy, Banacha 1, 02-097 Warszawa, Poland*

Received 10 June 2005; accepted 7 September 2005
Available online 29 September 2005

Abstract—The X-ray diffraction analysis of *N*-*p*-nitrophenyl-α-D-ribopyranosylamine (**1**) and *N*-*p*-nitrophenyl-α-D-xylopyranosylamine (**2**) was performed. It was found that an independent part of the unit cell of compound **1** is formed by three molecules of sugar whereas the crystals of compound **2** have one molecule in the independent part of the crystal unit cell. Additionally, **1** crystallizes with one molecule of water. The solvent molecule forms an extensive hydrogen bond network with the hydroxyl groups of the sugar, and this efficiently stabilizes the crystal lattice. Contrary to **2,** the sugar moieties of **1** adopt the $^1C_4$ conformation. In the spectra of **2**, *N*-*p*-nitrophenyl-2,3,4-tri-*O*-acetyl-β-D-lyxopyranosylamine and *N*-*p*-nitrophenyl-2,3,4-tri-*O*-acetyl-α-L-arabinopyranosylamine the number of resonances does not exceed the number of carbon atoms in the molecules, thus indicating no polymorphism. In the spectrum of (**1**) the signals are split, confirming the presence of three independent molecules in the crystal unit cell.

Keywords: Glycopyranosylamines; Crystal structure; ^{13}C NMR analysis; Solid-state NMR

1. Introduction

Glycopyranosylamines belong to an important group of biologically active compounds. Many of them include nucleic acids, glycoproteins, coenzymes, and some of the members of the vitamin B group, etc. Lai and Axelvod[1] found that some glycosylamines are strong inhibitors of glycosidases. Legler[2] and Legler and coworkers[3,4] claimed that *N*-substituents increased the inhibitory potency of some of the glycosylamines. But *N*-arylation of those compounds decreases the inhibitory potency of the above-mentioned derivatives.[2] Naturally occurring nucleosides can be classified as *N*-arylpentopyranosylamines. Many synthetic nucleosides possess therapeutical applications. For example, compounds like 1-β-D-arabinofuranosylcytosine (ara-C), 2′-deoxy-1-β-D-arabinofuranosyl 5-fluorouridine (FUdR), etc. have anticancer properties.[5] Among some nucleosides there are also antiviral agents like 9-β-D-arabinofuranosyladenine (ara-A), 1-β-D-ribofuranosyl-1,2,4-triazole-3-carboxamide (ribavirin), etc.[5] Also browning of foods caused by heating is sometimes connected with the presence of glycosylamines.[6]

2. Results and discussion

The *N*-*p*-nitrophenylglycopyranosylamines presented in Scheme 1 were prepared by the reaction of appropriate

* Corresponding author. Fax: +48 22 822 5996; e-mail: atemer@chem.uw.edu.pl

0008-6215/$ - see front matter © 2005 Elsevier Ltd. All rights reserved.
doi:10.1016/j.carres.2005.09.009

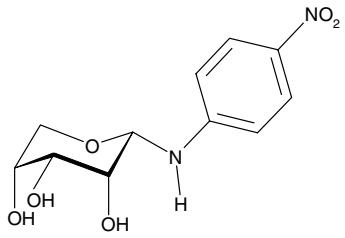

1

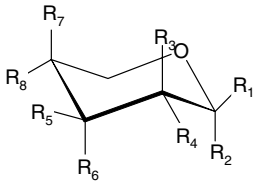

2 $R_1 = R_3 = R_5 = R_7 = H$, $R_2 = NH\text{-}C_6H_4\text{-}4\text{-}NO_2$, $R_4 = R_5 = R_8 = OH$

3 $R_2 = R_4 = R_6 = R_7 = H$, $R_1 = NH\text{-}C_6H_4\text{-}4\text{-}NO_2$, $R_3 = R_5 = R_8 = OAc$

4 $R_2 = R_3 = R_6 = R_8 = H$, $R_1 = NH\text{-}C_6H_4\text{-}4\text{-}NO_2$, $R_4 = R_5 = R_7 = OH$

Scheme 1.

monosaccharide with *p*-nitroaniline in water, ethanol, and glacial acetic acid on boiling water bath. Suitable crystals of *N*-*p*-nitrophenyl-α-D-ribopyranosylamine (**1**) and *N*-*p*-nitrophenyl-α-D-xylopyranosylamine (**2**) were obtained by slow crystallization from ethanol. The crystal structures of the two molecules (**1** and **2**) were determined in order to ascertain their stereochemistry and solid-state conformations. Those data as well as literature data of crystal structures of *N*-*p*-nitrophenyl-2,3,4-tri-*O*-acetyl-β-D-lyxopyranosylamine (**3**) and *N*-*p*-nitrophenyl-2,3,4-tri-*O*-acetyl-α-L-arabinopyranosylamine (**4**)[7] constituted a basis for solid state NMR studies. The configuration, conformation, and atom numbering of compounds **1** and **2** are shown in Figures 1 and 2.

Crystal data and structural refinement are specified in Table 1, whereas the bond lengths, bond angles and torsion angles, and hydrogen bonds for **1** and **2** are given in Tables 2–5. Both *N*-*p*-nitrophenyl-α-D-ribopyranosylamine (**1**) and *N*-*p*-nitrophenyl-α-D-xylopyranosylamine (**2**) crystallize in the $P2_12_12_1$ space group. An independent part of the unit cell is formed by three molecules of sugar in the former and one molecule in the latter case. Additionally, **1** crystallizes with one molecule of water, which is disordered into two positions with the occupancy factor of 0.5. As can be expected, the solvent molecule and the hydroxyl groups form an extensive hydrogen bond network, which efficiently stabilizes the

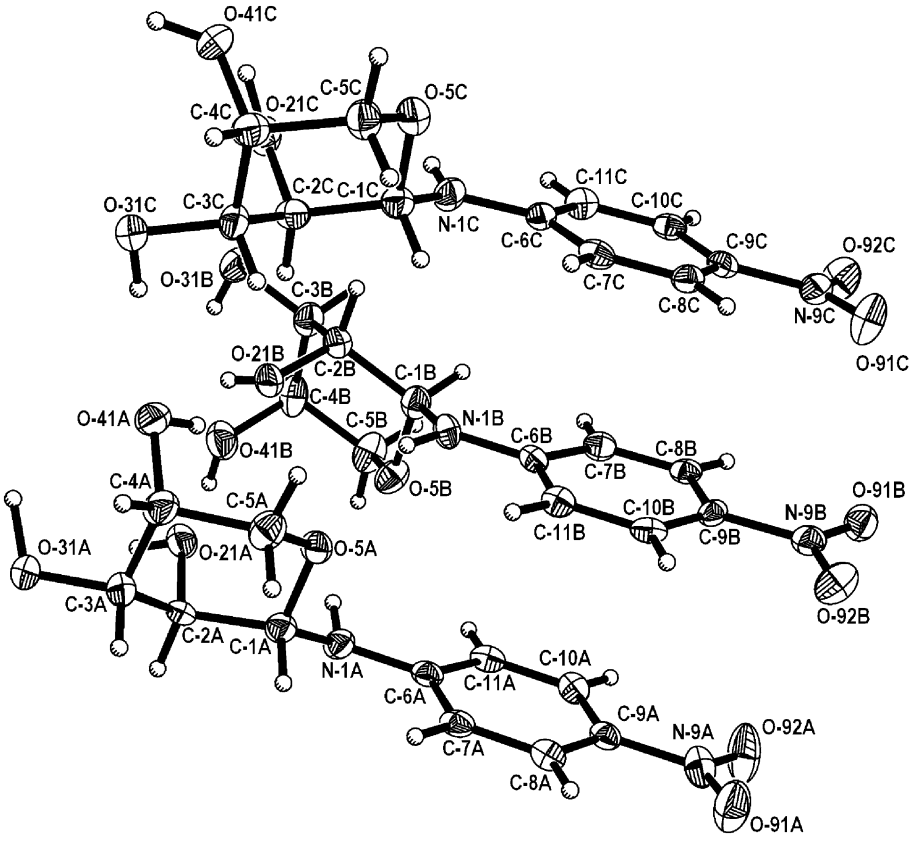

Figure 1. The ORTEP scheme and atom numbering of three molecules in an independent part of the unit cell of *N*-*p*-nitrophenyl-α-D-ribopyranosylamine (**1**) (the solvent molecule omitted for the clarity). The ellipsoids are drawn at the 50% probability level.

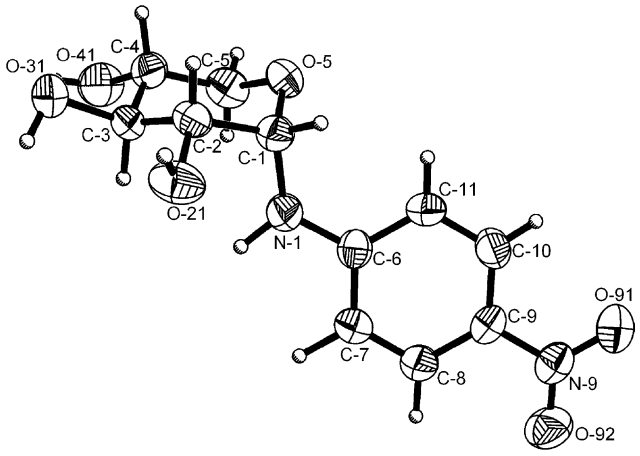

Figure 2. The ORTEP scheme and atom numbering of a molecule of *N*-*p*-nitrophenyl-α-D-xylopyranosylamine (**2**). The ellipsoids are drawn at the 50% probability level.

crystal lattice. The most significant ones, shown in Figure 3, involve the O-41C–H-41C···O-41B, O-31A–H-31A···O-21C, O-31C–H-31C···O-41A, O-21A–H-21A···O-31C, and O-41A–H-41A···O-21B interactions with the intermolecular distances between the oxygen atoms of 2.682(4) Å, 2.697(4) Å, 2.766(4) Å, 2.806(4) Å, 3.034(4) Å, respectively. The water molecule interacts with two hydroxyl groups at C-3B and C-4B at the distance (between the oxygen atoms) of ca. 2.7–2.8 Å.

The hydrogen bonds (as well as the other packing forces) led to a differentiation of the molecules of

Table 2. The bond lengths (Å) for *N*-*p*-nitrophenyl-α-D-ribopyranosylamine (**1**) and *N*-*p*-nitrophenyl-α-D-xylopyranosylamine (**2**)

Bond length	Compound			
	1A	**1B**	**1C**	**2**
C-1–N-1	1.440(4)	1.426(4)	1.427(4)	1.421(5)
C-1–O-5	1.444(4)	1.448(4)	1.433(4)	1.440(4)
C-1–C-2	1.522(5)	1.522(5)	1.519(5)	1.534(5)
C-2–O-21	1.435(4)	1.422(4)	1.446(4)	1.423(4)
C-2–C-3	1.524(5)	1.536(5)	1.530(5)	1.508(5)
C-3–O-31	1.438(4)	1.424(4)	1.433(4)	1.428(5)
C-3–C-4	1.516(5)	1.513(5)	1.525(5)	1.517(5)
C-4–O-41	1.436(4)	1.425(4)	1.438(4)	1.427(4)
C-4–C-5	1.531(5)	1.537(5)	1.525(5)	1.500(5)
C-5–O-5	1.439(4)	1.433(4)	1.441(4)	1.435(5)
N-1–C-6	1.388(4)	1.370(4)	1.372(4)	1.384(4)
C-6–C-11	1.397(5)	1.401(4)	1.401(4)	1.382(5)
C-6–C-7	1.402(4)	1.402(4)	1.418(5)	1.409(5)
C-7–C-8	1.378(5)	1.371(5)	1.362(5)	1.380(5)
C-8–C-9	1.389(4)	1.387(4)	1.386(4)	1.395(5)
C-9–C-10	1.396(5)	1.390(4)	1.381(4)	1.396(6)
C-9–N-9	1.453(4)	1.449(4)	1.445(4)	1.437(5)
N-9–O-91	1.238(4)	1.243(3)	1.233(4)	1.238(5)
N-9–O-92	1.221(4)	1.254(3)	1.235(4)	1.222(4)
C-10–C-11	1.381(5)	1.374(5)	1.386(5)	1.362(5)

Table 1. Crystal data and structure refinement for *N*-*p*-nitrophenyl-α-D-ribopyranosylamine (**1**) and *N*-*p*-nitrophenyl-α-D-xylopyranosylamine (**2**)

	Compound	
	1	**2**
Empirical formula	$3C_{11}H_{14}N_2O_6 * H_2O$	$C_{11}H_{14}N_2O_6$
Formula weight	864.75	270.24
Temperature (K)	100(2)	293(2)
Space group	$P2_12_12_1$	$P2_12_12_1$
Unit cell dimensions		
a (Å)	10.546(2)	6.361(1)
b (Å)	10.709(2)	9.100(2)
c (Å)	33.583(7)	19.991(4)
Volume (Å^3)	3792.8(1)	1157.2(4)
Z (molecules/cell)	4	4
$D_{calculated}$ (Mg/m^3)	1.472	1.551
Absorption coefficient (mm^{-1})	0.122	0.128
F(000)	1768	568
Crystal size (mm)	$0.4 \times 0.2 \times 0.2$	$0.3 \times 0.2 \times 0.2$
Θ range for data collection (°)	3.27–25.0	3.36–25.0
Limiting indices	$-12 \leqslant h \leqslant 10$	$-7 \leqslant h \leqslant 7$
	$-12 \leqslant k \leqslant 12$	$-10 \leqslant k \leqslant 10$
	$-39 \leqslant l \leqslant 39$	$-23 \leqslant l \leqslant 23$
Reflections collected	28,932	8901
Independent reflections	6624 [$R_{int} = 0.0701$]	2031 [$R_{int} = 0.0904$]
Data (restraints) parameters	6624/0/585	2031/0/178
Goodness-of-fit on F^2	0.992	1.012
Final *R* indices [$I > 2\sigma(I)$]	$R_1 = 0.0514$,	$R_1 = 0.0557$,
	$wR_2 = 0.1213$	$wR_2 = 0.1299$
R indices (all data)	$R_1 = 0.0634$	$R_1 = 0.0794$
	$wR_2 = 0.1277$	$wR_2 = 0.1452$
Extinction coefficient	0.0028(5)	0.032(6)
Largest differences, peak and hole (e/A^{-3})	0.483 and −0.303	0.217 and −0.206

Table 3. The bond angles for *N*-*p*-nitrophenyl-α-D-ribopyranosylamine (**1**) and *N*-*p*-nitrophenyl-α-D-xylopyranosylamine (**2**)

Bond angle	Compound			
	1A	**1B**	**1C**	**2**
N-1–C-1–O-5	108.2(2)	108.7(3)	108.8(3)	112.9(3)
N-1–C-1–C-2	113.2(3)	111.1(3)	110.6(3)	111.4(3)
O-5–C-1–C-2	110.5(3)	109.1(3)	110.2(3)	109.1(3)
O-21–C-2–C-3	107.8(3)	111.5(3)	108.6(3)	109.5(3)
O-21–C-2–C-1	112.3(3)	113.2(3)	112.5(3)	109.0(3)
C-3–C-2–C-1	108.0(3)	109.3(3)	108.2(3)	112.2(3)
O-31–C-3–C-4	112.1(3)	112.8(3)	110.3(3)	107.8(3)
O-31–C-3–C-2	109.4(3)	109.7(3)	111.5(3)	110.3(3)
C-2–C-3–C-4	114.2(3)	111.7(3)	110.7(3)	110.4(3)
O-41–C-4–C-5	112.0(3)	110.1(3)	109.0(3)	107.4(3)
O-41–C-4–C-3	111.4(3)	109.4(3)	110.6(3)	110.3(3)
C-5–C-4–C-3	108.4(3)	109.4(3)	108.5(3)	110.4(3)
O-5–C-5–C-4	109.7(3)	111.0(3)	110.6(3)	111.2(3)
C-5–O-5–C-1	111.9(2)	111.9(3)	112.0(2)	111.9(3)
C-6–N-1–C-1	120.2(3)	123.8(3)	123.6(3)	125.1(3)
C-11–C-6–N-1	121.8(3)	118.9(3)	120.0(3)	119.1(3)
N-1–C-6–C-7	119.9(3)	122.9(3)	122.0(3)	121.5(3)
C-11–C-6–C-7	118.2(3)	118.1(3)	118.0(3)	119.4(4)
C-8–C-7–C-6	121.4(3)	121.0(3)	120.3(3)	119.7(4)
C-7–C-8–C-9	119.1(3)	119.6(3)	120.7(3)	119.5(4)
C-8–C-9–C-10	121.2(3)	120.7(3)	120.6(3)	120.7(3)
C-10–C-9–N-9	118.6(3)	119.1(3)	120.5(3)	118.6(4)
C-8–C-9–N-9	120.2(3)	120.2(3)	118.9(3)	120.7(4)
O92–N-9–O-91	123.5(3)	122.2(3)	122.6(3)	122.1(4)
O-91–N-9–C-9	117.9(3)	119.0(3)	119.4(3)	118.5(4)
O-92–N-9–C-9	118.6(3)	118.7(3)	118.0(3)	119.4(4)
C-10–C-11–C-6	121.4(3)	121.2(3)	121.2(3)	121.5(4)

Table 4. The torsion angles for *N*-*p*-nitrophenyl-α-D-ribopyranosylamine (**1**) and *N*-*p*-nitrophenyl-α-D-xylopyranosylamine (**2**)

Torsion angle	Compound			
	1A	**1B**	**1C**	**2**
N-1–C-1–C-2–O-21	−55.3(3)	−51.9(4)	−56.7(3)	50.9(4)
O-5–C-1–C-2–O-21	66.2(3)	67.9(3)	63.6(3)	176.2(3)
N-1–C-1–C-2–C-3	−176.9(3)	−177.9(3)	−179.1(3)	−70.5(4)
O-5–C-1–C-2–C-3	−55.4(3)	−58.1(3)	−58.8(3)	54.8(4)
O-21–C-2–C-3–O-31	59.7(3)	54.9(4)	59.7(3)	68.6(4)
C-1–C-2–C-3–O-31	178.4(2)	179.9(3)	179.7(3)	−170.3(3)
O-21–C-2–C-3–C-4	−66.8(4)	−70.9(4)	−63.4(3)	−172.3(3)
C-1–C-2–C-3–C-4	51.9(4)	54.0(4)	56.5(3)	−51.2(4)
O-31–C-3–C-4–O-41	−54.1(4)	−55.5(4)	−59.8(3)	−69.4(4)
C-2–C-3–C-4–O-41	71.0(4)	68.6(4)	64.0(3)	170.0(3)
O-31–C-3–C-4–C-5	–177.5(3)	−175.8(3)	−179.4(3)	172.1(3)
C-2–C-3–C-4–C-5	−52.4(4)	−51.6(4)	−55.5(3)	51.5(4)
O-41–C-5–C-5–O-5	−67.7(4)	−65.8(4)	−63.8(3)	−177.4(3)
C-3–C-4–C-5–O-5	56.1(4)	55.0(4)	56.7(3)	−57.1(4)
C-4–C-5–O-5–C-1	−63.9(3)	−62.2(4)	−61.5(3)	62.8(4)
N-1–C-1–O-5–C-5	−171.5(2)	−175.1(3)	−176.1(3)	64.3(4)
C-2–C-1–O-5–C-5	64.2(3)	63.6(3)	62.5(3)	−60.2(4)
O-5–C-1–N-1–C-6	68.1(4)	84.3(4)	83.2(4)	81.2(4)
C-2–C-1–N-1–C-6	−169.1(3)	−155.7(3)	−155.7(3)	−155.6(4)
C-1–N-1–C-6–C-11	−157.6(3)	−170.8(3)	−178.3(3)	172.4(3)
C-1–N-1–C-6–C-7	24.4(5)	11.2(5)	2.8(5)	−7.7(6)
N-1–C-6–C-7–C-8	179.1(3)	177.1(3)	177.3(3)	179.3(3)
C-11–C-6–C-7–C-8	1.0(5)	−1.0(4)	−1.7(5)	−0.8(5)
C-6–C-7–C-8–C-9	−0.4(5)	1.1(5)	1.3(5)	1.3(5)
C-7–C-8–C-9–C-10	−0.3(5)	0.0(5)	0.0(5)	−2.1(6)
C-7–C-8–C-9–N-9	178.5(3)	−179.8(3)	178.9(3)	177.5(3)
C-8–C-9–N-9–O-92	176.5(3)	−178.5(3)	176.8(3)	178.4(4)
C-10–C-9–N-9–O-92	−4.7(5)	1.6(4)	−4.3(4)	−1.9(5)
C-8–C-9–N-9–O-91	−4.1(5)	1.0(4)	−3.2(4)	−1.0(5)
C-10–C-9–N-9–O-91	174.6(3)	−178.8(3)	175.7(3)	178.6(4)
C-8–C-9–C-10–C-11	0.3(5)	−1.3(4)	−0.8(4)	2.4(6)
N-9–C-9–C-10–C-11	−178.4(3)	178.6(3)	−179.7(3)	−177.2(3)
C-9–C-10–C-11–C-6	0.3(5)	1.4(5)	0.4(4)	−1.9(6)
N-1–C-6–C-11–C-10	−179.1(3)	−178.4(3)	−178.1(3)	−179.0(4)
C-7–C-6–C-11–C-10	−1.0(5)	−0.3(5)	0.8(5)	1.1(6)

Table 5. Hydrogen bonds in *N*-*p*-nitrophenyl-α-D-ribopyranosylamine (**1**) and *N*-*p*-nitrophenyl-α-D-xylopyranosylamine (**2**)

Donor D–H	Acceptor A	*d*(D···H)	*d*(H···A)	<DHA
Compound **1**				
O-41C–H-41C	O-41B	1.8578	2.6824	164.33
O-31A–H-31A	O-21C	1.6430	2.6967	155.27
O-31C–H-31C	O-41A	1.8820	2.7657	157.35
O-21A–H-21A	O-31C	2.8058	2.0103	172.68
O-41A–H-41A	O-21B	3.0343	2.2179	153.10
Compound **2**				
O-31–H-31	O-5	2.7926	2.0684	147.09
O-21–H-21	O-41	2.8224	1.6832	169.19
O-41–H-41	O-92	3.0349	2.3746	138.12
N-1–H-1N	O-31	3.1859	2.3335	141.97

N-*p*-nitrophenyl-α-D-ribopyranosylamine. This involves a twist between the aromatic and sugar rings: C-1–N-1–C-6–C-11 (−157.6°, −170.8°, −178.3°, for molecules **1A**, **1B**, and **1C**, respectively) and C-1–N-1–C-6–C-7 (24.4°, 11.2°, 2.8°, for molecules **1A**, **1B**, and **1C**, respectively), the torsion angles in the glycosidic fragment O-5–C-1–N-1–C-6, (68.1°, 84.3°, 83.2°, for molecules **1A**, **1B**, and **1C**, respectively) and C-2–C-1–N-1–C-6 (−169.1°, −155.7°, −155.7°, for molecules **1A**, **1B**, and **1C**, respectively) and finally the torsion angles involving all hydroxyl groups. These differences are reflected in the Cremer and Pople puckering parameters estimated for sugar fragments.[8] The sugar moieties adopt the $^{1}C_{4}$ conformation, which is always slightly distorted. The Θ is equal to 174.6°, 175.4°, and 178.7° while the other puckering parameters Q and φ are equal to 0.578, 0.580, 0.592, and 175.05°, 212.45°, 246.63°, respectively for molecules **1A**, **1B**, and **1C**.

Also, the *N*-*p*-nitrophenyl-α-D-xylopyranosylamine (**2**) is involved in many H-bond interactions, as shown in Figure 4. The shortest bonds exist between the hydroxyl group at C-3 and the sugar O-5 (with the distance O···O of 2.793(4) Å) and between the hydroxyl group O-21–H-21 and O-41 (with the distance O···O of 2.822(4) Å). The other intermolecular interactions present in the crystal structure involve O-41–H-41···O-92 and N-1–H-1···O-31 with the distances between the non-hydrogen atoms of 3.035(4) and 3.186(4) Å, respectively. The sugar ring adopts slightly distorted $^{4}C_{1}$ conformation with the Cremer and Pople puckering parameters[8] $\Theta = 4.5°$ and $\varphi = 349.16°$ ($Q =$ 0.563 Å).

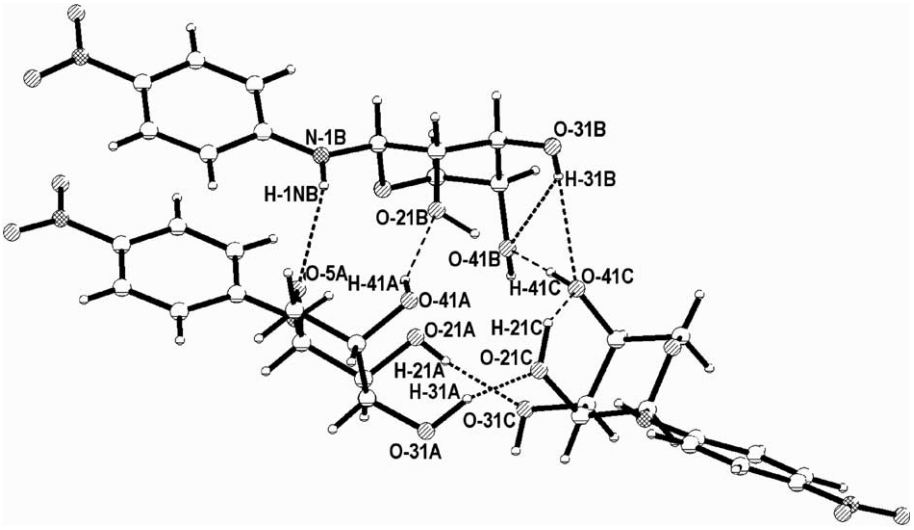

Figure 3. The intermolecular interactions in the crystal lattice for *N*-*p*-nitrophenyl-α-D-ribopyranosylamine (**1**).

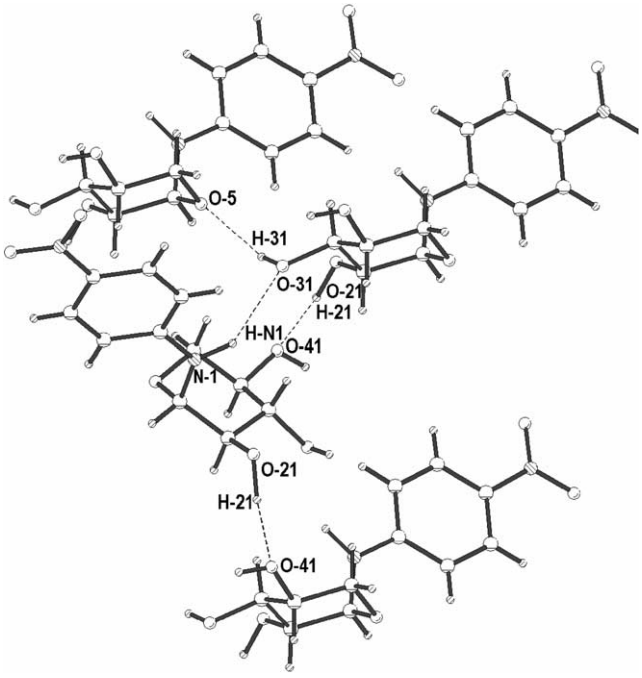

Figure 4. The intermolecular interactions in the lattice of *N*-*p*-nitrophenyl-α-D-xylopyranosylamine (**2**).

The one- and two-dimensional ^{1}H and ^{13}C NMR spectra for $CDCl_3$ solutions of **3**–**4** and DMSO-d_6 solutions of **1**–**2** were recorded and analyzed in order to obtain reliable assignment of ^{13}C resonances. The spectra for solids were recorded using cross-polarization (CP) magic angle spinning (MAS) technique and the ^{13}C CP MAS NMR spectra of *N*-*p*-nitrophenyl-2,3,4-tri-*O*-acetyl-β-D-lyxopyranosylamine (**3**) is illustrated in Figure 5.

Chemical shifts were assigned on the basis of liquid-state ones. However, some solid-state resonances had significantly different chemical shifts than their liquid-state counterparts. These resonances were assigned following the same sequence as the calculated shielding constants. The ^{13}C NMR chemical shifts for glycosylamines **1**–**4** are collected in Table 6. In the spectra of **2**, **3**, and **4** the number of resonances does not exceed the number of carbon atoms in the molecules, indicating no polymorphism. In the spectrum of *N*-*p*-nitrophenyl-α-D-ribopyranosylamine (**1**) (Fig. 6), the signals are split, confirming the presence of three independent molecules in the crystal unit cell. The intensity of C-1_{Ph}, C-4_{Ph}, and C-1 resonances are 2:1 indicating that one molecule (**1A**) exhibits significantly different geometry than the other two. The most significant differences are related to the twist angles of the aromatic ring. The angle C-1–N-1–C-6–C-11 is −157.6° in **A** whereas it is −170.8° and −178.3° in **1B** and **1C**, respectively. Similarly, the angle O-5–C-1–N-1–C-6 of 68.1° can be found in **1A**, that is less by 16° than the angles 84.3° (**1B**) and 83.2° (**1C**). The geometry of the NO_2 group is almost coplanar with the aromatic ring (within ±3.6°). The assignment of resonances to the respective carbons in the molecules **1A**, **1B**, and **1C** is rather tentative, and based on signal intensities.

Compounds **3** and **4** have the NH group as hydrogen bond donor, and the NH···O bond could be expected involving the proximal oxygen atom of sugar moiety. However, it is not possible to realize an intramolecular hydrogen bond with the hydrogen at N-1 (**3** and **4**). This proton is closed in a cage made of surrounding phenyl and acetyl group at C-2. The replacement of hydrogen at N-1 by a sterically bigger acetyl group at N-1 breaks the cage and another conformation appears.[7] In structurally similar compounds,[9] the nitro group was isolated from the hydrogen bonding pattern established by the sugar hydroxyl groups. The tendency toward isostructuralism has been observed among pyranosylamines with

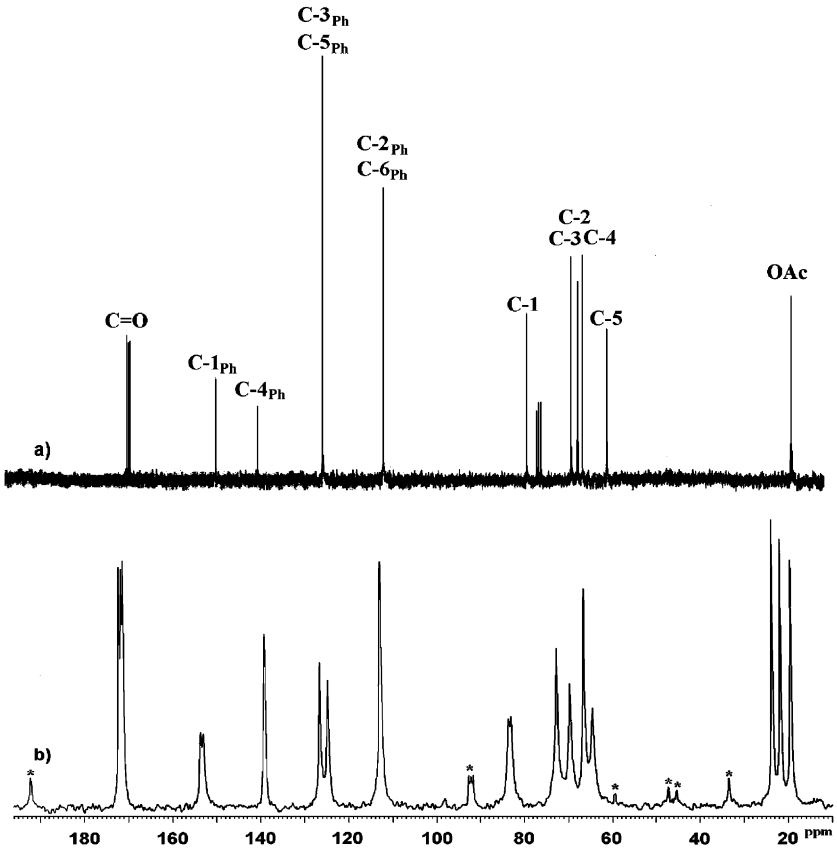

Figure 5. ^{13}C NMR spectra *N*-*p*-nitrophenyl-2,3,4-tri-*O*-acetyl-β-D-lyxopyranosylamine (**3**), (a) in $CDCl_3$ and (b) in solid state (*: spinning side band).

Table 6. ^{13}C NMR data (δ in ppm)[a] in DMSO-d_6 for *N*-*p*-nitrophenyl-α-D-ribopyranosylamine of (**1**), *N*-*p*-nitrophenyl-α-D-xylopyranosylamine (**2**), and in $CDCl_3$ for *N*-*p*-nitrophenyl-2,3,4-tri-*O*-acetyl-β-D-lyxopyranosylamine (**3**) and *N*-p-nitrophenyl-2,3,4-tri-*O*-acetyl-α-L-arabinopyranosylamine (**4**)

Atom	**1**						**2**			**3**			**4**		
	A			B											
	δ_{liquid}	δ_{solid}	Δ[b]	δ_{liquid}	δ_{solid}	Δ	δ_{liquid}	δ_{solid}	Δ	δ_{liquid}	δ_{solid}	Δ	δ_{liquid}	δ_{solid}	Δ
C-1	80.70	82.66	2.0	80.70	80.71		80.28	81.06		80.06	83.72/83.14	3.7/3.1	83.66	82.04	−1.6
C-2	69.48	70.90	1.4	69.48	70.90	1.4	70.43	69.09	−1.34	68.37	66.57	−1.8	69.08	72.78	3.7
C-3	69.74	70.90	1.2	69.74	70.90	1.2	71.74	74.44	2.7	70.27	72.88	2.6	70.40	69.83	
C-4	67.70	70.90	3.2	67.70	70.90	3.2	69.39	69.09		66.95	69.87	2.9	68.07	68.17	
C-5	63.39	58.24	−5.1	63.39	68.24	4.8	62.75	60.11	−2.6	61.99	64.64	2.6	64.98	65.57	
$C\text{-}1_{Ph}$	152.9	153.1		152.9	150.7	−2.2	153.4	151.5	−1.9	150.4	153.7/153.1	3.3/2.7	150.4	152.4	2.0
$C\text{-}2_{Ph}$	112.6	114.0	1.4	112.6	109.3	−3.3	112.6	111.6	−1.0	113.4	112.8		113.1	117.0	3.9
$C\text{-}3_{Ph}$	125.8	125.8		125.8	123.2	−2.6	125.6	125.0		126.2	124.7	−1.5	126.0	129.9	3.9
$C\text{-}4_{Ph}$	137.5	138.6	1.1	137.5	136.6		137.4	139.2	1.8	140.4	138.9	−1.5	140.2	140.1	
$C\text{-}5_{Ph}$	125.8	125.8		125.8	123.2	−2.6	125.6	128.0	2.4	126.2	126.5		126.0	126.2	
$C\text{-}6_{Ph}$	112.6	114.9	2.3	112.6	110.8	−1.8	112.6	117.3	4.7	113.4	112.8		113.1	109.9	−3.2

[a] Protecting groups not included.
[b] $\Delta = \delta_{solid} - \delta_{liquid}$; Δ <1 was omitted.

the *p*-nitrophenyl substituent. In a series of *N*-aryl compounds (non-acetylated) no significant differences in bond length (O-5–C-1) have been observed. An exception was the *p*-NO_2 substituted derivative in which delocalization of the electron pair from the glycosidic nitrogen into the aryl ring has been suggested.[9] The nitro group of non-acetylated compounds does not participate in hydrogen bonding.

The signals of carbons linked to nitrogen atoms are slightly broader and split into doublets due to the resid-

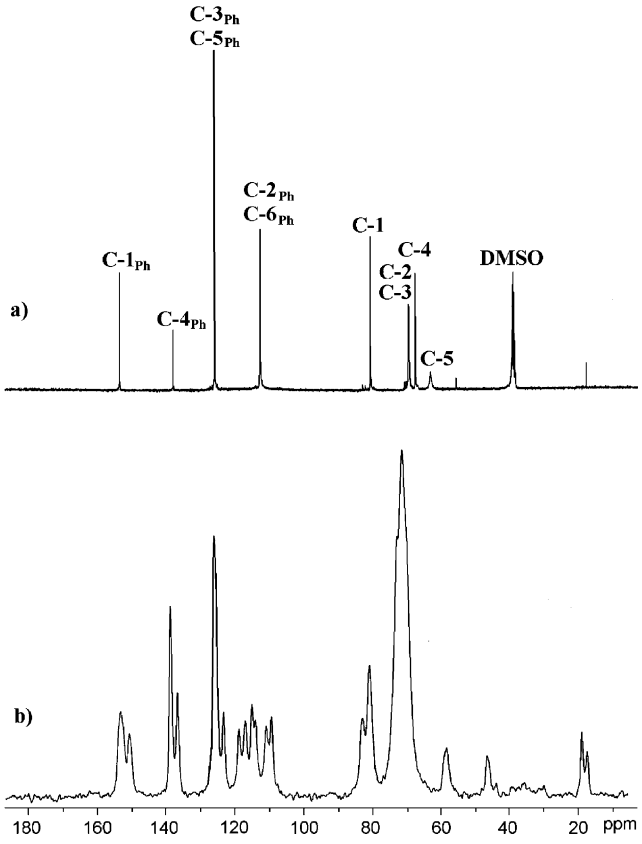

Figure 6. ^{13}C NMR spectra *N*-*p*-nitrophenyl-α-D-ribopyranosylamine (**1**), (a) in DMSO-d_6 and (b) in solid state.

ual ^{13}C–^{14}N quadrupolar coupling, enabling fast identification of C-1$_{Ph}$–N, N–C-1 resonances. The dynamics of cross-polarization in **1**–**4** is effective and the spectra of reasonable quality (Fig. 5) can be obtained within half an hour (ca. 800 scans).

Chemical shift differences can result from crystal packing as well as from conformational differences. The values of $\Delta\delta$ 2.5–3.7 ppm are observed for sugar carbons in **3** and of −3.8 to 2.0 ppm for aromatic carbons in **4**.

Separate signals of *ortho* and *meta* carbons of the phenyl ring were observed in the CP MAS spectra of **1**–**4** and the assignment of those resonances was not obvious. Therefore, the calculations of optimal geometry and NMR shielding constants were performed for compounds **2**, **3**, and **4**, and the results are collected in Table 7.

The shielding of C-2$_{Ph}$ and C-6$_{Ph}$ was sensitive to the twist angle of the aromatic ring and the geometry of the glycosidic linkage.

The calculated shielding constants (σ values) for all carbons in the molecules **2**, **3**, and **4** were compared with the respective ^{13}C CP MAS NMR chemical shifts (δ, ppm), enabling more reliable assignments of C-2$_{Ph}$, C-6$_{Ph}$ as well as C-3$_{Ph}$, C-5$_{Ph}$ pairs.

Linear relationships [σ (ppm) = $a * \delta_{CPMAS} + b$] were obtained and the equation parameters a, b and correlation coefficients are included in Table 7. The best agreement (Fig. 7) between experimental δ and theoretical σ values was achieved for (isolated) *a* molecule with C-1–N-1–C-6–C-11 angle of 158°. The reverse assignment of C-2$_{Ph}$ and C-6$_{Ph}$ resonances results in lesser agreement.

Table 7. The isotropic ^{13}C NMR shielding constants calculated by DFT GIAO method for *N*-*p*-nitrophenyl-α-D-xylopyranosylamine (**2**), *N*-*p*-nitrophenyl-2,3,4-tri-*O*-acetyl-β-D-lyxopyranosylamine (**3**), and *N*-*p*-nitrophenyl-2,3,4-tri-*O*-acetyl-α-L-arabinopyranosylamine (**4**), and correlation parameters and coefficients

Atoms	**2**	**3**	**4**
C-1	99.76	106.49	105.95
C-2	113.70	120.95	115.79
C-3	114.72	118.48	119.66
C-4	118.72	119.28	124.09
C-5	121.04	130.42	131.41
C-1$_{Ph}$	41.52	44.75	46.92
C-2$_{Ph}$	81.71	76.97	82.20
C-3$_{Ph}$	69.54	70.24	69.16
C-4$_{Ph}$	52.70	52.14	52.87
C-5$_{Ph}$	69.91	70.05	69.13
C-6$_{Ph}$	78.70	74.56	82.76
a	−0.8521	−0.9432	−0.9186
b	174.72	186.08	185.55
R^2	0.9827	0.9887	0.9868

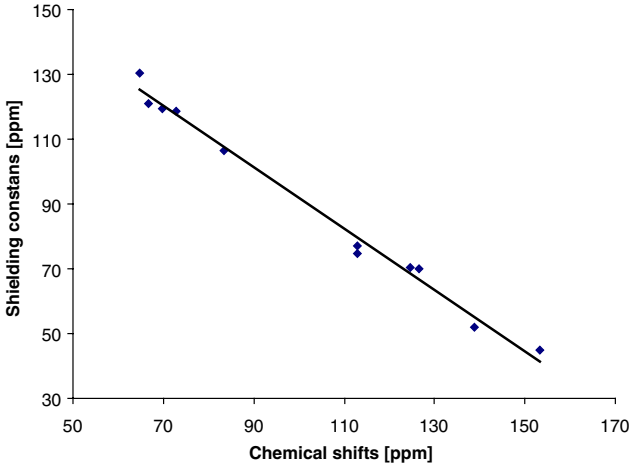

Figure 7. The plot of calculated shielding constants σ (ppm) and experimental chemical shifts δ (ppm) for *N*-*p*-nitrophenyl-2,3,4-tri-*O*-acetyl-β-D-lyxopyranosylamine.

3. Experimental

A general method for synthesis of *N*-*p*-nitrophenylglycopyranosylamines was already described.[10–12] Compounds **3** and **4** were synthesized according to Smiatacz[13] and Sokołowski.[12]

3.1. *N*-*p*-Nitrophenyl-α-D-ribopyranosylamine (1)

Yellow crystals, yield, 73%; mp 110–112 °C, $[\alpha]_D^{20}$ +332.9 (Pyridine), lit.[11] 178 °C; $[\alpha]_D^{20}$ +349 (Pyridine).

3.2. *N*-*p*-Nitrophenyl-α-D-xylopyranosylamine (2)

Yellow crystals, yield, 59%; mp 185–189 °C, $[\alpha]_D^{20}$ +232.2 (EtOH), lit.[13] 188 °C; $[\alpha]_D^{22}$ +280 (EtOH).

3.3. *N*-*p*-Nitrophenyl-2,3,4-tetra-*O*-acetyl-β-D-lyxopyranosylamine (3)

Yellow crystals, yield, 72%; mp 205–208 °C, $[\alpha]_D^{20}$ −193.9 ($CHCl_3$), lit.[12] mp 209–210 °C; $[\alpha]_D^{23}$ −189 ($CHCl_3$).

3.4. *N*-*p*-Nitrophenyl-2,3,4-tetra-*O*-acetyl-α-L-arabinopyranosylamine (4)

Yellow crystals, yield, 70%; mp 172–173 °C, $[\alpha]_D^{20}$ +0.6 ($CHCl_3$), lit.[13] mp 172–176 °C; $[\alpha]_D^{23}$ +4 ($CHCl_3$), erroneously for this compound configuration β was ascribed.

3.5. Physical measurements

The X-ray diffraction measurements of *N*-*p*-nitrophenyl-α-D-ribopyranosylamine (**1**) and *N*-*p*-nitrophenyl-α-D-xylopyranosylamine (**2**) were performed on a KUMA CCD κ-axis diffractometer with graphite-monochromated MoKα radiation (0.71073 Å) at 100 ± 2 and 293 ± 2 K, respectively. The crystals of the latter compound (**2**) were unstable when cooling, therefore a room-temperature measurement was performed. It is the reason of significantly bigger thermal ellipsoids in this case. The crystals were positioned at 62.3 mm from the KM4CCD camera. Six hundred and sixty-four frames were measured at 0.9° intervals with a counting time of 35 s, 600 frames were measured at 1.0° intervals with a counting time of 30 s, respectively. Data collection, cell refinement, and data reduction were carried out with the Kuma Diffraction programs: CrysAlis CCD and CrysAlis RED.[14] The data were corrected for Lorentz and polarization effects, but no absorption correction was applied. The structures were solved by direct methods[15] and refined using SHELXL.[16] The enantiomers were assigned by reference to an unchanging chiral center in the synthetic procedure. The refinement was based on F^2 for all reflections except for those with very negative F^2. The weighted R factor, wR and all goodness-of-fit S values are based on F^2. The non-hydrogen atoms were refined anisotropically while the hydrogen atoms were placed in the calculated positions. The positions and the thermal parameters of the hydrogen atoms participating in hydrogen bonds were refined isotropically. The atomic scattering factors were taken from the International Tables.[17]

The ^{1}H and ^{13}C NMR spectra for DMSO-d_6 solutions were recorded on a Bruker DRX-400 MHz spectrometer, the 2D experiments were run using standard Bruker software. Cross polarization magic angle spinning solid-state ^{13}C NMR spectra were recorded at 100.1 MHz on Bruker DRX-400 MHz spectrometer. Powder samples were spun at 8 kHz in 4 mm ZrO_2, contact time of 4–5 ms, repetition time of 8 s and spectral width of 25 kHz were used for accumulation of 200–600 scans. Chemical shifts were calibrated indirectly through the glycine CO signal recorded at 176.0 ppm, relative to TMS.

Semi-empirical PM3 calculations were performed to obtain the minimum energy conformations. For the calculations of NMR shielding constants the DFT-GIAO with the 6-31G** basis set approach was used from Gaussian 98 package.[18] The calculations were performed on a Silicon Graphic Origin200 (2xR 10,000) workstation.

4. Supplementary material

Full crystallographic details, except the structure features, have been deposited with the Cambridge Crystallographic Data Centre. These data may be obtained, on request, from The Directory, Cambridge Crystallographic Data Centre, 12 Union Road, Cambridge, CB2 1EZ, UK (fax: +44-1223-336033; e-mail: deposit@ccdc.cam.ac.uk or www: http://www.csdc.cam.ac.uk). Deposition numbers CCDC 274143 (**1**) CCDC 274144 (**2**).

Acknowledgments

Financial support from Warsaw University (BST-972/14/2004) is gratefully acknowledged. The X-ray measurements were undertaken in the Crystallographic Unit of the Physical Chemistry Laboratory at the Chemistry Department of the University of Warsaw.

References

1. Lai, H. Y. L.; Axelvod, B. *Biochem. Biophys. Res. Commun.* **1973**, *54*, 463–468.
2. Legler, G. *Biochem. Biophys. Acta* **1978**, *524*, 94–101.
3. Legler, G.; Sinnott, M. L.; Withers, S. G. *J. Chem. Soc., Perkin Trans. 2* **1980**, 1376–1383.
4. Legler, G.; Herrchen, M. *Carbohydr. Res.* **1983**, *116*, 95–103.
5. Kennedy, J. F. *Carbohydrate Chemistry*; Clarendon Press: Oxford, 1988, pp 177–183.
6. Danehy, J. P.; Pigman, W. W. *Adv. Food Res.* **1951**, *13*, 241.
7. Dukurno, P.; Łubkowski, J.; Myszka, H.; Smiatacz, Z. *Z. Kristallogr.* **1994**, *209*, 808–812.
8. (a) Cremer, D.; Pople, J. A. *J. Am. Chem. Soc.* **1975**, *97*, 1354–1358; (b) Cremer, D. *Acta Crystallogr., Sect. B* **1984**, *40*, 498–500.
9. Ojala, C. R.; Ostman, J. M.; Hanson, S. E.; Ojala, W. H. *Carbohydr. Res.* **2001**, *332*, 415–427.

10. Weygand, F.; Perkow, W.; Kuhner, P. *Chem. Ber.* **1951**, *84*, 594–602.
11. Douglas, J. G.; Honeyman, J. *J. Chem. Soc.* **1955**, 3674–3680.
12. Sokołowski, J.; Paszkiewicz, E. *Polish J. Chem.* **1979**, *53*, 305–316.
13. Smiatacz, Z.; Sokołowski, J. *Roczniki Chem.* **1970**, *44*, 757–767.
14. Oxford Diffraction. CrysAlis CCD and CrysAlis RED. Oxford Diffraction Poland, Wrocław, Poland; 2001.
15. Sheldrick, G. M. Phase annealing in SHELX90: direct methods for larger molecules. *Acta Cryst.* **1990**, *A46*, 467–473.
16. Sheldrick, G. M. SHELXL93. *Program for the Refinement of Crystal Structure*; University of Göttingen: Germany, 1993.
17. *International Tables for Crystallography*; Wilson, A. J. C., Ed.; Kluwer: Dordrecht, 1992; Vol. C.
18. Frisch, M. J.; Trucks, G. W.; Schlegel, B.; Scuseria, G. E.; Robb, M. A.; Cheeseman, J. R.; Zakrzewski, V. G.; Montgomery, J. A., Jr.; Stratmann, R. E.; Burant, J.; Dapprich, C. S.; Millam, J. M.;. Daniels, A. D.; Kudin, K. N.; Strain, M. C.; Farkas, O.; Tomasi, J.; Barone, V.; Cossi, M.; Cammi, R.; Mennucci, B.; Pomelli, C.; Adamo, C.; Clifford, S.; Ochterski, J.; Petersson, G. A.; Ayala, P. Y.; Cui, Q.; Morokuma, K.; Malick, D. K.; Rabuck, A. D.; Raghavachari, K.; Foresman, J. B.; Cioslowski, J.; Ortiz, J. V.; Baboul, A. G.; Stefanov, B. B.; Liu, G.; Liashenko, A.; Piskorz, P.; Komaromi, I.; Gomperts, R.; Martin, R. L.; Fox, D. J.; Keith, T.; Al-Laham, M. A.; Peng, C. Y.; Nanayakkara, A.; Gonzalez, C.; Challacombe, M.; Gill, P. M. W.; Johnson, W. B.; Chen, W.; Wong, M. W.; Andres, J. L.; Gonzalez, C.; Head-Gordon, M.; Replogle, E. S.; Pople, J. A.; Gaussian 98. Revision A.7. Gaussian, Pittsburgh, PA, 1998.